MEASURING THE HEAT TRANSFER COEFFICIENT IN A DIRECT OIL-COOLED ELECTRICAL MACHINE USING THIN FILM HEAT FLUX GAUGES

Conference Paper · September 2015

CITATIONS
5

READS
365

4 authors:

Robert Camilleri
University of Malta
27 PUBLICATIONS **200** CITATIONS
SEE PROFILE

Paul Beard
University of Oxford
39 PUBLICATIONS **324** CITATIONS
SEE PROFILE

David Howey
University of Oxford
155 PUBLICATIONS **4,862** CITATIONS
SEE PROFILE

Malcolm D. Mcculloch
University of Oxford
224 PUBLICATIONS **4,922** CITATIONS
SEE PROFILE

MEASURING THE HEAT TRANSFER COEFFICIENT IN A DIRECT OIL-COOLED ELECTRICAL MACHINE USING THIN FILM HEAT FLUX GAUGES

R. Camilleri*[1], P. Beard[2], D. A. Howey[3] and M. D. McCulloch[4]

[1] *Energy and Power Group, Dept. of Eng. Sci., University of Oxford, UK, robert.camilleri@eng.ox.ac.uk*
[2] *Osney Thermo-Fluids Lab., Dept. of Eng. Sci., University of Oxford, UK, paul.beard@eng.ox.ac.uk*
[3] *Energy and Power Group, Dept. of Eng. Sci., University of Oxford, UK, david.howey@eng.ox.ac.uk*
[4] *Energy and Power Group, Dept. of Eng. Sci., University of Oxford, UK,* malcolm.mcculloch@eng.ox.ac.uk

Abstract

This paper presents the measurement of the heat transfer coefficient (HTC) in an oil-cooled electrical machine with a segmented stator using double layered heat flux gauges. While heat flux gauges have been used for HTC measurements in applied to aerospace components such a gas turbine blades, to the authors knowledge the technique has never been applied to directly oil-cooled electrical machines. Therefore the paper explores the challenges linked with this technique when applied to this setting. The paper develops a correlation for the HTC on the sides of the pole pieces and compares the non-dimensional Nusselt number with existing correlations for laminar flow in pipes.

Keywords: heat transfer coefficient, thin film gauges, directly oil-cooled electrical machine

Nomenclature

Roman Symbols

D_h	hydraulic diameter (m)
h	heat transfer coefficient (W/m^2 K)
I	current (A)
k	thermal conductivity (W/m K)
L	length of pipe (m)
Nu	Nusselt number
P	Heat load (W)
$\dot{q}$	heat flux (W/ m^2)
R	electrical resistance (Ω)
R_{iso}	reference electrical resistance at isothermal temperature T_{iso} (Ω)
R_o	reference electrical resistance at T_0 (Ω)
T	temperature (^{o}C)
T_{iso}	isothermal reference temperature (^{o}C)
T_o	reference temperature at T_0 (typically 0 ^{o}C)
V	voltage (V)
u	uncertainty
x	substrate insulation thickness (m)

Greek Symbols

α	temperature coefficient (K)
α_e	temperature coefficient of resistance, α/R_{ref} (Ω/K)

Subscript

block	substrate block value
sub_b	at the bottom of insulation substrate
sub_t	at the top of insulation substrate
iso	isothermal
ref_fluid	reference fluid temperature

INTRODUCTION

The quest to improve the current density in electrical machines requires both the electromagnetic and thermal aspects of the machine to be optimized. As the winding insulation is rated to a maximum operating temperature the hottest spot in the stator windings limits the machine life and torque ratings. Therefore accurate thermal modelling of the machine allows proper choice of material, avoids unnecessary derating and reduces safety factors thus ensuring that high torque densities are achieved. Thermal modelling is often performed using lumped parameter models (Mellor et al., 1991, Boglietti et al., 2009). These are fast to solve but require input parameters such as the heat transfer coefficient (HTC). The HTC is often found by CFD simulation (Howey, 2010, Airoldi, 2010, Wrobel et al., 2015) or experimental measurements (Howey et al, 2011, Hettegger et al, 2012). Despite the higher current density of liquid cooled electrical machines and the importance to produce accurate thermal models, to the authors' knowledge no experimental research that measures the heat transfer coefficient in liquid cooled machines exist. This is therefore the subject of this paper, which fills this gap by applying thin film heat flux gauges to measure the HTC in a direct oil-cooled electrical machine. The paper is organised in the following manner: The geometrical boundary conditions for this problem is first described by presenting the electrical machine used as a test case study. A brief overview of the measuring technique using thin film gauges is then presented, after which the gauge manufacturing and calibration procedure is outlined. Finally the experimental procedure undertaken is described, from which the HTC values are derived.

DIRECT LIQUID COOLED ELECTRICAL MACHINES

Air-cooled machines suffer from thermal limitations (Camilleri, et al., 2012). While the heat transfer in the rotor-stator gap can be improved by introducing an evaporative cooling mechanism as shown in (Camilleri, et al., 2015), the thermal path is still restricted by heat transfer from fins in the machine casing. This thermal limit does not exist in liquid cooled machines because the heat transfer is augmented by the extended surfaces of an external radiator. Therefore in high current density electrical machines such as those required in electric and hybrid vehicles, liquid cooling is often preferred. This is often achieved by wrapping a cooling jacket around the casing of the machine. Even higher current densities are however achieved by having the liquid oil in direct contact with the windings. Fig. 1 shows an example of this cooling configuration for an axial flux machine. The machine is made from a segmented stator through which the oil is distributed. Thermal modeling of this machine requires that the heat transfer coefficient on the surface of each segment is known.

Thin film gauges: Application to an oil cooled electrical machine

Thin film heat flux gauges are a type of film resistance measuring device. The change in electrical resistance of a platinum sensor that is sputtered onto an insulating substrate is measured. The electrical resistance of the gauges, R, is dependent on temperature and can be described by the linear relationship:

$$R = R_o + \alpha.(T - T_o) \quad (1)$$

R_o is a known reference resistance at a reference temperature T_o, generally 0 ^{o}C. α is a temperature coefficient describing the change in film resistance with temperature. The product of α and R_{ref} provides the temperature coefficient of resistance, α_e, at temperature T_{ref}. The surface temperature is therefore inferred by the change in electrical resistance and the gauge parameters, which are derived following an initial calibration process.

The high frequency response (100 kHz) of the thin film gauges has made them suitable for transient techniques in gas turbine applications, (Jones et al. 1995). Test times are typically 10 μs to 1s, during which a pulse of hot air is passed over the test piece and the change in voltage across the gaige whilst supplied with a constant current, is recorded. The time history of voltage is then used to determine the change is gauge resistance, and hence temperature, with respect to time. The calculation of heat flux from the temperature history can be performed in a number of methods, for example the impulse response method documented by Oldfield, 2008. Finally, the convective heat transfer coeficient (HTC) and adiabatic wall temperature (allowing for compressibility effects) is determined from a linear regeression of heat flux and driving temperature. In this research, the double-layered thin film gauge shown in Fig. 2 is used to determine the HTC. In the context of an oil-cooled component, the large thermal capacity of the oil cooling system makes the transient impulse response unsuitable. The technique presented here is modified from the transient method in that the metal substrate is heated until a steady state condition is reached. The metal substrate temperature was measured by two k-type bare-bead thermocouples located on the upper and lower walls.

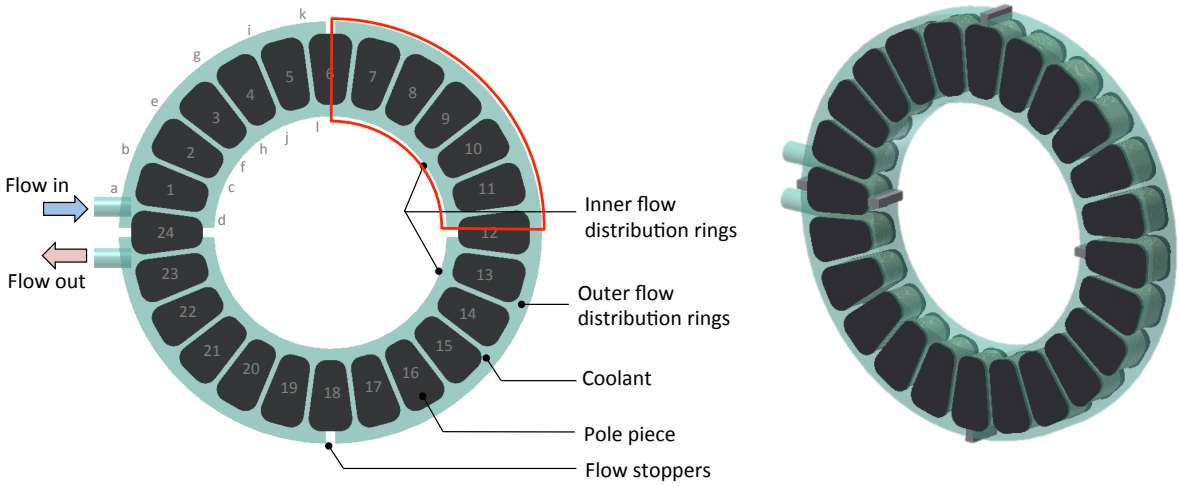

Fig. 1. Schematic of a direct liquid cooled segmented stator for an axial flux machine. (Highlighted) quarter segment replicated in experiments

These measurements agreed to within 0.5K showing the block was isothermal during testing. Steady state heat flux was determined using the one-dimensional Fourier conduction equation across the insulating substrate:

$$\dot{q} = \left({}^{k}/_{x}\right)\left(T_{subs\_b} - T_{subs\_t}\right) \tag{2}$$

in which $\dot{q}$ is the heat flux through the sensor, x is the thickness of the polyimide insulating layer separating the two gauges, k is the thermal conductivity of polyimide, T_{subs_t} and T_{subs_b} are the temperatures at the top and bottom surfaces of the polyimide insulating layer respectively. Test were conducted over a range of substrate temperatures and a linear regression of heat flux against $(T_{block} - T_{fluid\ ref})$ performed to determine the convective heat transfer coefficient. $T_{fluid\ ref}$ is a fluid temperature to which the HTC is referenced. The heat transfer coefficient is therefore found from:

$$\dot{q} = h = \left(T_{block} - T_{fluid\ ref}\right) \tag{3}$$

To determine the heat flux and hence the heat transfer coefficient, the thermal properties of the heat flux gauges are also required. The thermal properties of the polyimide and glue layers used are well documented by the manufacturers and have very similar properties, and such can be regarded as one material. The thermal properties of the substrate between the heat flux gauges are shown in Table 1. The fluid reference temperature used to define the heat transfer coefficient should theoretically be the local bulk fluid temperature. However, the difficulty in measuring the local fluid temperature often results in the heat transfer coefficient being defined using an alternative reference fluid temperature. On measuring the HTC on the stator of an air cooled machine, Howey, 2010, and Wrobel et al., 2015, chose the bulk air inlet temperature in a the rotor-stator gap as their reference temperature. Airoldi et al., 2008, used the temperature at the centre of the rotor-stator gap. This paper uses the oil inlet temperature as the reference. The oil inlet temperature is measured by two thermocouples.

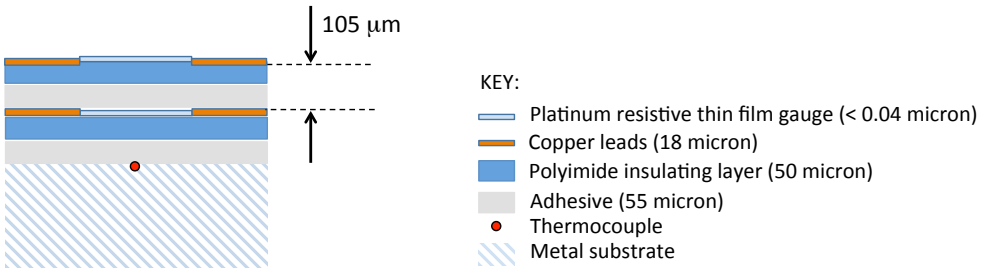

Fig. 2. Schematic showing a) Direct Heat Flux Gauge, b) Double sided Direct Heat Flux Gauge

Table 1: Measured substrate material properties

Property	Thermal conductivity, k (W/m K)	Thickness, x (m)	$\left(k/x\right)$
	0.46	1.05e-6	4380

MANUFACTURING AND CALIBRATION OF THIN FILM HEAT FLUX GAUGES

The temperatures T_{subs_t} and T_{subs_b} are derived from the measured resistances of the thin film gauges on top and below the insulation substrate. It was shown in eqn. (1) how calculating each of these temperatures requires the values of R_o and α. These values are found by calibrating the gauges at isothermal conditions for a range of working temperatures. A reference temperature sensor that gives a calibrated temperature measurement is used, thus:

$$R_{calib} = R_o + \alpha . T_{calib} \tag{4}$$

As the gauge parameters are affected by the manufacturing and mounting process, calibration is performed after the thin film gauges are mounted on the test piece. The gauges were manufactured at the fabrication facility of thin film gauges at the Osney Thermo-fluids Laboratory at the University of Oxford. Details of the fabrication process of thin film gauges are found in (Collins et al., 2015). A pole piece replica was manufactured in aluminium and instrumented with eight double-layered thin film gauges on each side of the oil flow channel, as shown in Fig. 3. Aluminium was chosen due to its high conductivity, which aids uniform heating of the segmented pole pieces, and ease of manufacturing. The calibration process was also performed at the Osney Thermo-Fluids Laboratory using a bespoke calibration facility. The facility uses a measurement system based on National Instruments PXI systems with a thermostatically controlled water bath. The water bath temperature is interfaced through a serial interface and a relay switch module is controlled by a Labview script and allows to measure up to 96 resistances simultaneously. During the calibration process, the instrumented test piece was sealed in a plastic bag and placed in a water bath. The water bath temperature was increased from 20 ^{o}C to 45 ^{o}C in steps of 5 ^{o}C. The pole piece temperature and water bath temperature were monitored to ensure isothermal conditions. These temperatures and resistances of the thin film gauges were recorded. The linear relationship of each gauge resistance was plotted against the known set of temperatures. This allows the extraction of the temperature coefficient α and reference resistance R_o for each gauge. An example of a typical calibration chart for one thin film heat flux gauge is shown in Fig. 4.

While for platinum α is found to experience very little variation with temperature and is considered constant, R_o sometimes experiences a drift (Collins et al., 2015). This is mainly in high temperature environments synonymous with aerospace components, and is likely due to induced stresses and relaxation of the gauge connections. However, although the measurements presented in this research are low temperature (<100 ^{o}C), steady state experiments take longer to settle. The complete set of tests presented here, were performed over a few days. Therefore to counter for any possible drift in R_o during the course of the testing period, an isothermal test was performed at the start of each measured data set. Hence, during the experiment, temperature of the each gauge was determined as a function of the calibration parameter α and measured parameters R, R_{iso} and T_{iso}:

$$T = \left(\frac{R - R_{iso}}{\alpha}\right) + T_{iso} \tag{5}$$

EXPERIMENTAL WORK

Assessment of the pole piece heating system

The steady state experiment required the aluminium test piece to be heated. To assess this, the heating system was simulated in Autodesk CFD Simulation. A three-dimensional model of the aluminium block with heater was designed and meshed. The cartridge heater was set to be stainless steel and was set to produce a heat generation of 80 W. A thermal contact resistance of 0.3 K/W was applied between the heater and the aluminium block to represent the thermal grease. The presence of the polyamide layer on the heat flux gauges was simulated through an additional resistance at the solid-fluid boundary.

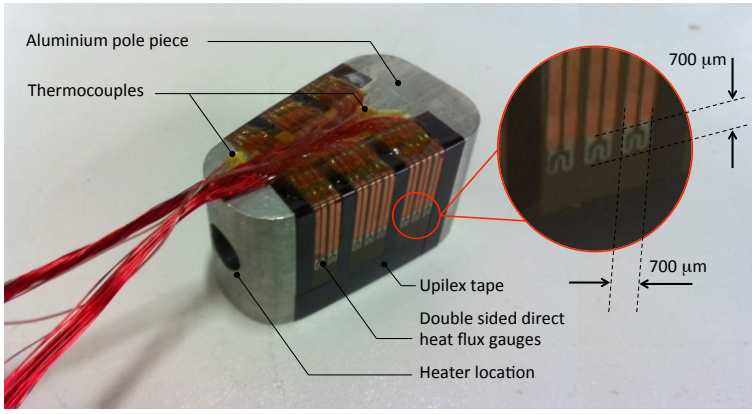

Fig. 3. Aluminium test piece with mounted direct heat flux gauges.

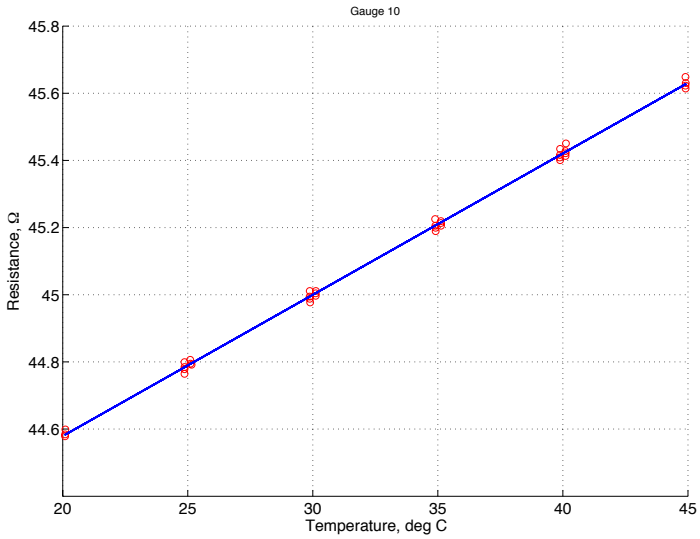

Fig. 4. Example of a calibration chart for a thin film gauge, from which the values of temperature coefficient α and reference resistance R_o (y-intersect at T=0 °C) for each gauge is determined.

An estimated convective heat transfer coefficient of 200 W/m^{2}K was prescribed on the solid-fluid surface. The external temperature of the aluminium block is presented in Fig. 2. It can be seen that a surface temperature of 85 °C is reached with a variation of less then 1 °C on the instrumented surface. The model sensitivity to the thermal resistance presented by the polyamide layer was also checked in the simulation. The temperature distribution remains unchanged and therefore this heating method was deemed suitable.

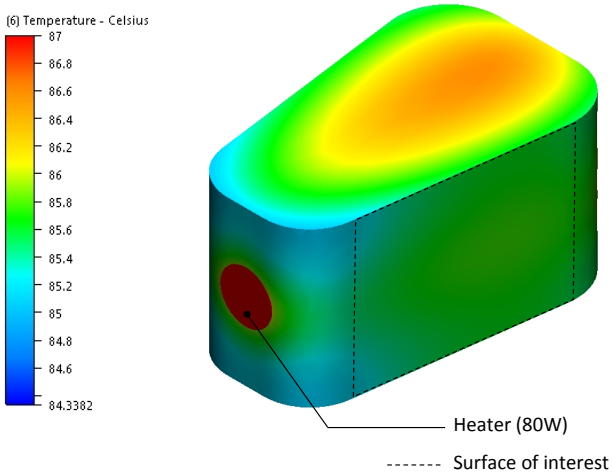

Fig. 5. Simulation of the segmented pole piece to assess the heating system of the pole piece.

Experimental setup

Segmented stators offer the benefit of undertaking thermal analysis on single pole pieces rather than the whole machine stator (Wrobel et al, 2011). This significantly simplifies thermal experiments speeding up the thermal design of the machine. In this work, a representative experiment of a quadrant of the stator highlighted in Fig. 1. was set up. Six pole piece replicas were machined in aluminium and used to replace the segmented stator pole pieces. Each pole piece was fitted with a 230 V, 150 W cartridge heater of dimensions 10 mm diameter x 50 mm length. The heater simulates the total internal heat generation in each pole piece. Silicone based thermal interface material was applied to improve the heat transfer between the heater and the pole pieces. Each pole piece was drilled with two 1mm holes and fitted with two thermocouples. These were used to monitor the temperature variation in the metal body. The pole pieces were carefully assembled on a plastic base in a test box, recreating the flow channels between them as shown in Fig. 6. The plastic base acts as a thermal insulator and limits the heat transfer to the test box.

The pole piece heaters were connected to a variable transformer, which was used to regulate the heat input to the pole piece, thus varying the surface temperature of the pole pieces. Current meters and a differential voltage probe were used to measure the current and voltage supplied to the heaters using a PicoScope 3000 series oscilloscope recording at 1 Hz. The heat input P was calculated as:

$$P = I.V \tag{6}$$

I is the d.c. measured current and V the and V the d.c. voltage supplied to the heaters. This was used to double-check the energy balance across the test piece. Pico data loggers were used to record pole piece temperatures at 1 Hz. The oil was re-circulated from a reservoir into the test rig and then pumped through a heat exchanger, expelling heat to ambient. The reservoir was also fitted with a heating element to control the inlet temperature of the fluid into the test section. The power input to the oil reservoir heater was also regulated through a transformer. The flow rate was regulated using a globe valve and measured using a variable area flow meter. A Schematic of the test rig is shown in Fig. 7. A test matrix shown in Table 2 was performed for flow rates between 1 lpm and 6 lpm. Oil inlet temperatures were varied between 25 ^{o}C and 45 ^{o}C and pole piece surface temperature between 30 ^{o}C to 80 ^{o}C, in steps of 10 ^{o}C. Each experiment was run for 1-3 hours, until steady state conditions were achieved. The steady state values across the final hour were then averaged to determine the oil inlet temperature and the pole piece body temperatures. The gauges resistances were measured from which the temperature difference across the Upilex substrate were determined.

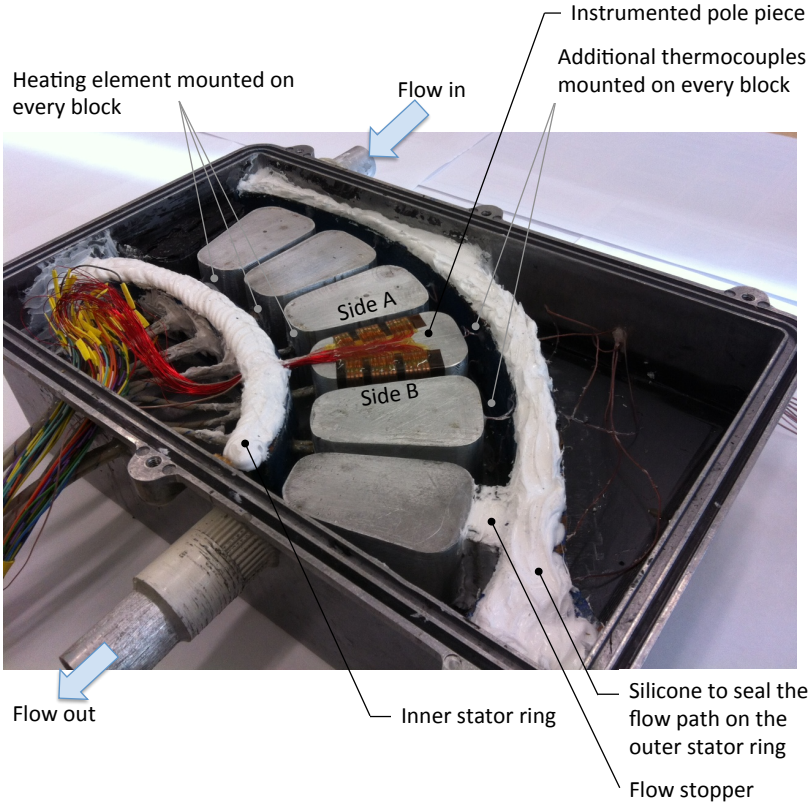

Fig. 6. Test box showing a section of the stator machine and instrumented pole piece

Table 2: Test Matrix for oil flow rates of between 1 and 6 lpm

Oil inlet temperature ^{o}C	**Pole piece temperature** ^{o}C					
25	30	40	50	60	70	80
35		40	50	60	70	80
45			50	60	70	80

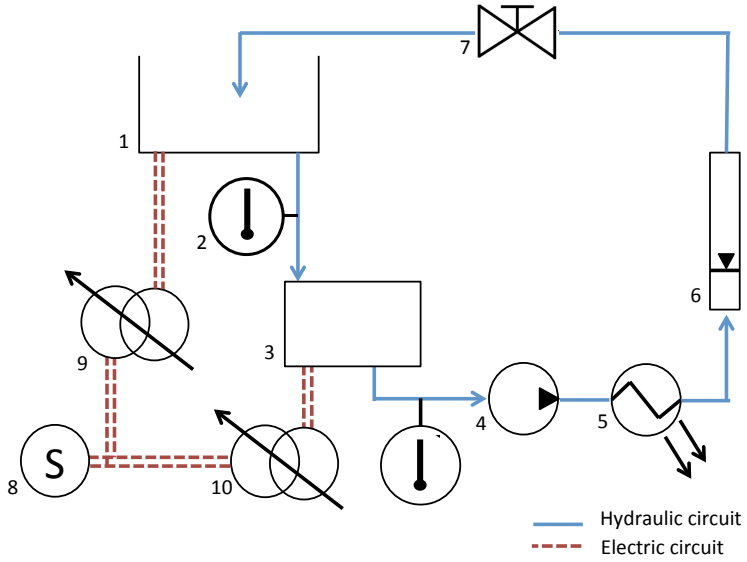

Fig. 7. Test setup with 1) oil reservoir, 2) temperature sensors, 3) test box, 4) pump, 5) heat exchanger, 6) variable area flow meter, 7) globe valve, 8) ac power supply, 9) variable transformer to power fluid heater, 10) variable transformer to power pole piece heaters.

Calibration of the temperature sensors

The thermocouples measuring the metal and fluid temperature were also calibrated in a water bath. The thermocouples and data acquisition system were calibrated against a reference PT100 temperature sensor with a known absolute calibration accuracy of +/- 0.05 K, for a range of temperatures from 20 ^{o}C to 180 ^{o}C. The oven hysteresis was measured at 0.1 K, while the thermocouple offset was measured at 0.33 K.

Calibration of the flow meter

The flow rate in the experiment was measured using a variable area flow meter. These are calibrated for water. Therefore a recalibration process to account for the density and viscosity of oil at various operating temperatures was required. The calibration by weight method shown in standards APTI435 and ISA-RPI16.6-1961 was used. The setup is shown in Fig. 8. With the position of the flow meter noted, the mass of fluid collected was measured and timed. The calibration process was repeated for a number of oil inlet temperatures. A relationship for the flow rate with float position at different temperatures was derived.

Uncertainty Analysis

The temperature sensor uncertainty *u(T)* was calculated using:

$$u(T) = \sqrt{[u(T_{\mathrm{TC}})]^2 + [u(T_{\mathrm{RT}})]^2 + [u(T_{\mathrm{OH}})]^2} \tag{7}$$

In which the $u(T_{\mathrm{TC}})$ is the thermocouple offset, $u(T_{\mathrm{RT}})$ is the reference temperature accuracy and $u(T_{\mathrm{OH}})$ is the oven hysteresis. The temperature uncertainty was calculated to be 0.35 K. The uncertainty in the voltage meter $u(V)$ was $\pm 0.2\ V$ while the uncertainty in the current meter $u(I)$ was $\pm 0.01\ mA$. The uncertainty of the heat load u(P) was calculated as:

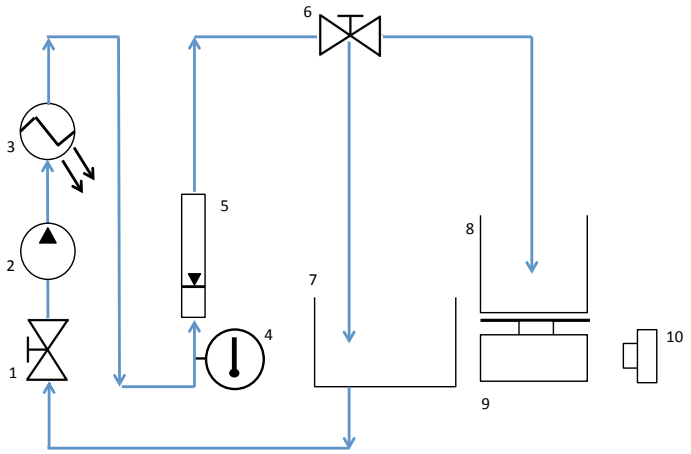

Fig. 8. Schematic showing flow meter calibration by mass using 1) gate valve, 2) pump, 3) heat exchanger, 4) thermometer, 5) flow meter, 6) 3-way valve, 7) reservoir, 8) collecting beaker, 9) scales, 10) video camera

$$\mathrm{u(P)} = \sqrt{[u(V).I]^2 + [u(I).V]^2} \tag{8}$$

The uncertainty of heat input was found to be 4 mW at low heat flux and 33 mW at the high heat flux. The uncertainty of the calibration scales was 1mg with a reading error of 0.01g. The stopwatch used in the flow calibration has an uncertainty $u(t)$ of $\pm 0.1\ s$. The uncertainty in the flow meter $u(Q_{fm})$ was 0.1 lpm. Hence the uncertainty in flow rate measurement $\mathrm{u(Q)}$ was calculated at:

$$\mathrm{u(Q)} = \sqrt{[u(Q).t]^2 + [u(t).Q]^2 + \left[u(Q_{fm})\right]^2} \tag{9}$$

The uncertainty of the measured flow rate is $\pm 0.114\ lpm$.

TEST RESULTS AND DISCUSSION

Post Processing the Gauge Data

For each flow rate and oil inlet temperature, the gauge resistances vs. pole piece block temperature was plotted, thus ensuring that the thin film gauges behaved as expected with their resistance increasing with temperature. An example for one test is shown in Fig 9. By plotting the linear relationship of the temperature difference across the insulation substrate against the block temperature, the consistency of the gauges was checked. It was generally noted that at a low temperature difference between the oil and the block temperature the gauge readings do not follow the linear trend. An example of this is shown in Fig. 10 These points were discarded in the calculation of the heat transfer coefficient as they may result in a high uncertainty. A MATLAB script was developed in which eqns. (2)-(7) are solved to determine the local heat flux and local HTC values. An example of the local HTC values is shown in Fig. 11. The reference to side A and side B is indicated in Fig. 6.

Correlation of the Mean HTC Values

While the experiment provides a map of the local heat transfer coefficient along the pole piece sides for various oil inlet flow rates and temperatures, an average value for each side of the pole piece was calculated. This was used to derive a correlation of the HTC with Reynolds number. Fig 12 shows a correlation of the HTC on pole pieces sides A and B with inlet Reynolds number. It can be noted how side A experience higher HTC values than side B. To establish a correlation with the properties of the flow in the channels adjacent to the instrumented sides, the flow distribution within the stator quarter was established using a flow network model for the segmented stator topology. The flow model was presented in (Camilleri et al., 2015). The Reynolds number for each flow channel adjacent to sides A and B was therefore calculated and correlated to the measured HTC for each respective side as shown in Fig 13. To compare the measurements with existing correlations, the non-dimensional Nusselt number *Nu,* was defined as:

$$Nu = \frac{hD_h}{k} \tag{10}$$

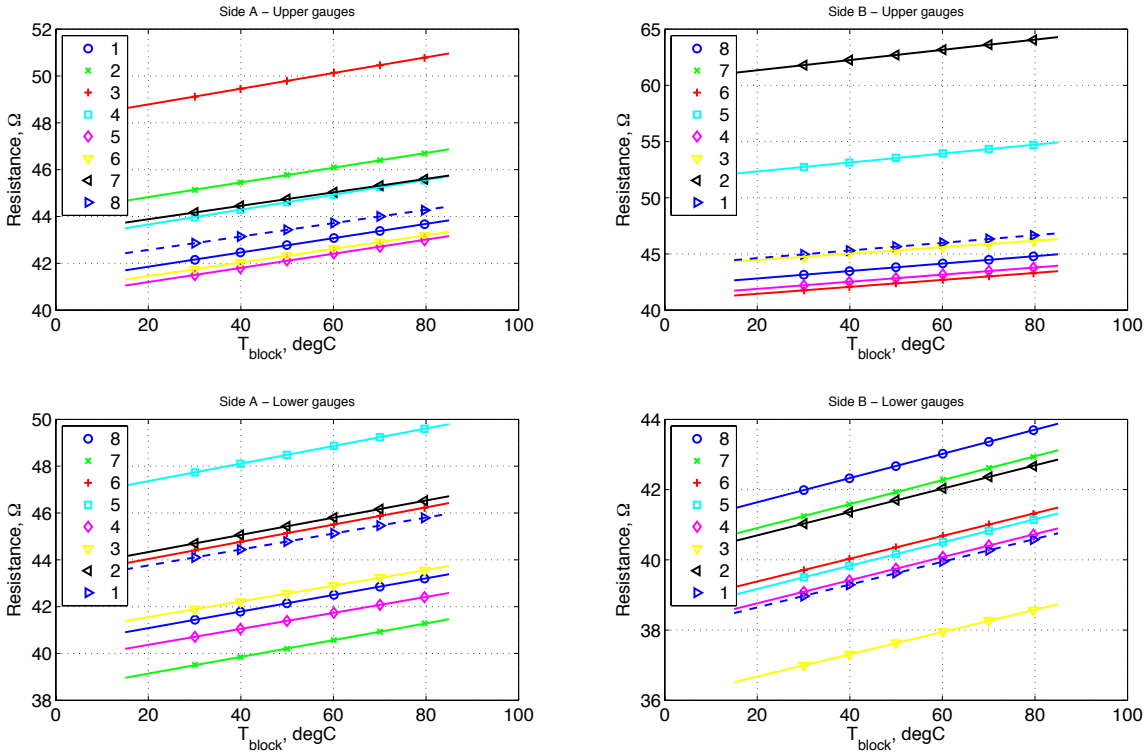

Fig. 9. Variation of gauge resistances with pole piece block temperature

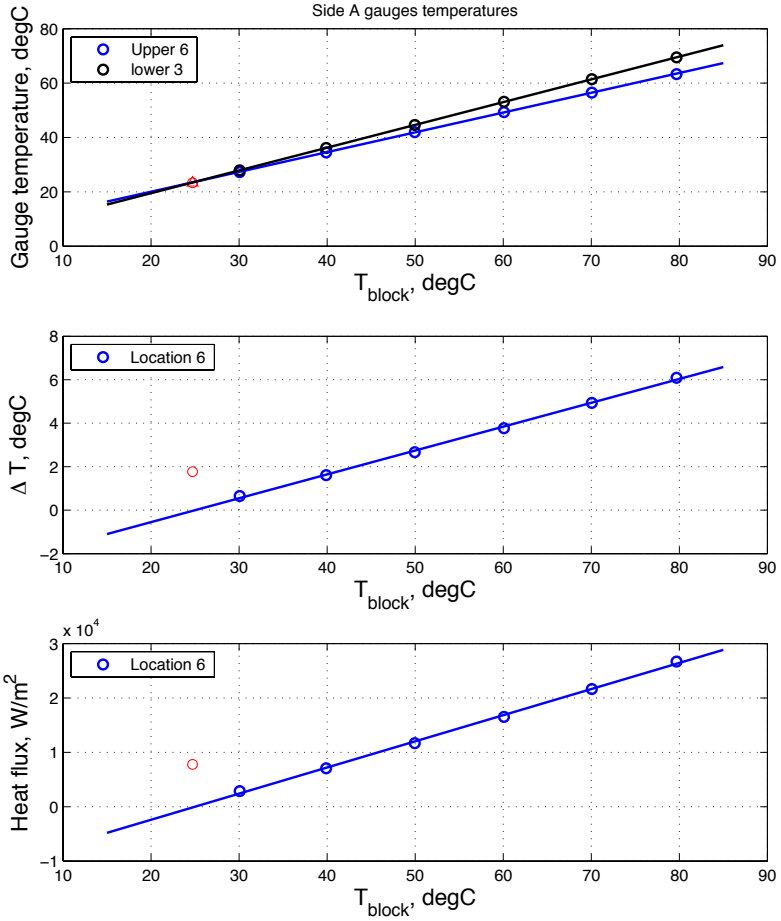

Fig. 10. (Top) Variation of the gauge temperature with pole piece temperature, (Middle) Linear variation of the temperature difference across the insulation substrate with block temperature. The offset temperature in red is ignored during the processing of the gauges. (Bottom) Linear variation of the heat flux across the gauges with block temperature.

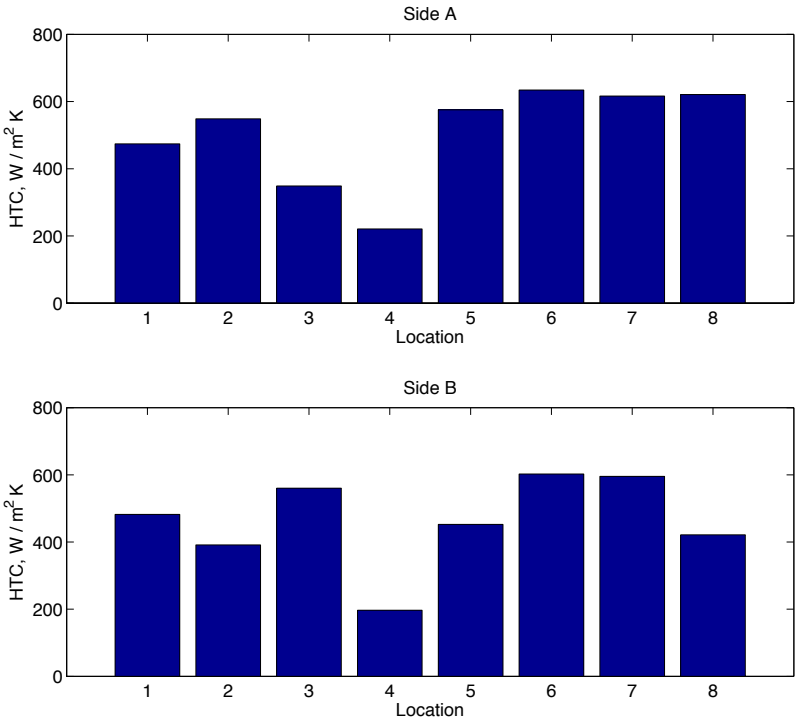

Fig. 11. Example of the local HTC values on sides A and B of the pole piece

The Nu was correlated with the channel Reynolds number such that $Nu = a\,Re^{b}$, as shown in Fig 14. In which the coefficients a is 25.12 for side A and 15.407 for side B respectively and b is 0.042 for side A and 0.1212 for side B respectively. The Nu for laminar flow in short pipes and developing thermal and fluid boundary layer can be determined using the Seider Tate equation:

$$Nu_{S-T} = 1.86(Pr\ Re\ )^{0.33}(D_{\mathrm{h}}\ )^{0.33}\left(\frac{\mu_b}{\mu_w}\right)^{0.14} \tag{11}$$

Or for laminar flow of fluids with Prandtl no. > 5 and developing hydrothermal boundary layer:

$$Nu_{Pr>5} = \left(\frac{\mu_b}{\mu_w}\right)^{0.14}\left[3.66 + \frac{0.0668\,Pr\,Re\,\left(\frac{D_{\mathrm{h}}}{L}\right)}{1 + 0.04\left(Pr\,Re\,\left(\frac{D_{\mathrm{h}}}{L}\right)\right)^{0.667}}\right] \text{ for } \mathrm{Pr} > 5 \tag{12}$$

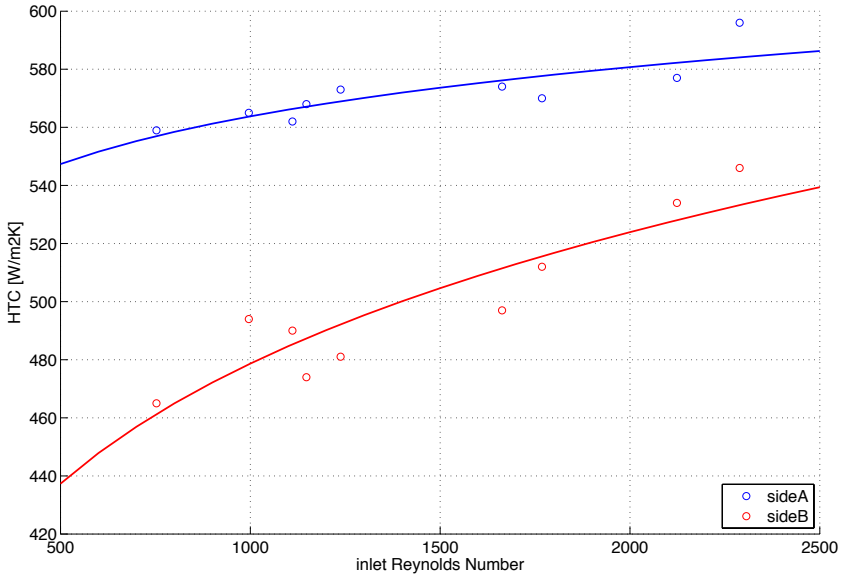

Fig. 12. Example of the mean HTC for the two sides of the pole piece with inlet Reynolds number

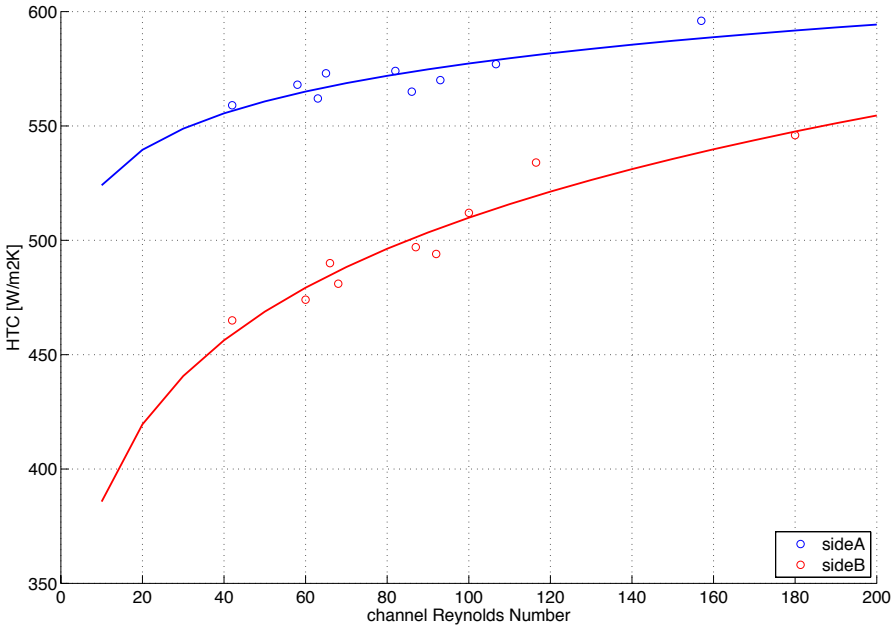

Fig. 13. Example of the mean HTC for the two sides of the pole piece with channel Reynolds number

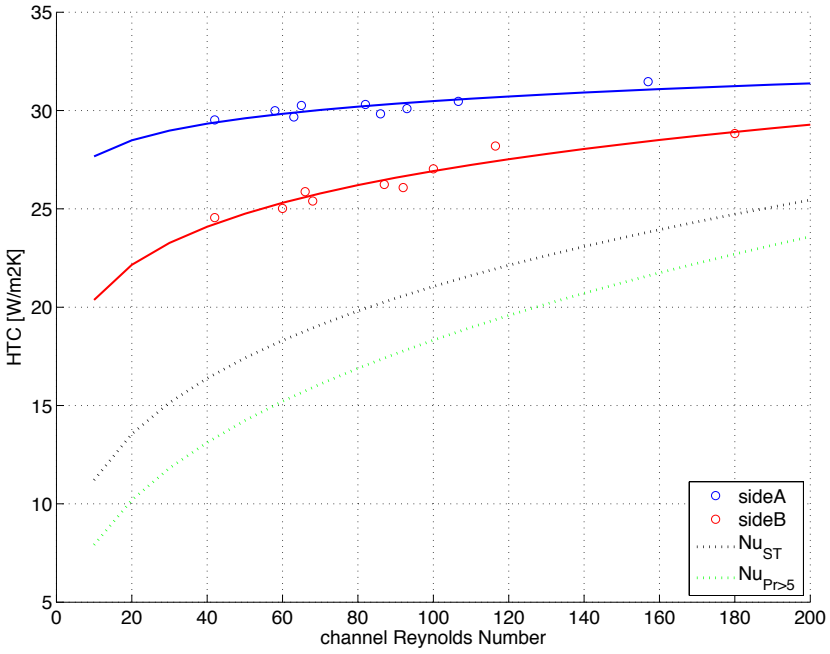

Fig. 14. Comparison of the measured non-dimensional Nusselt number to existing correlations

CONCLUSION

This paper presents a method for measuring the heat transfer coefficient in a directly oil cooled electrical machine with segmented stator using the double layered heat flux gauges. The measrement were correlated with the Reynolds number along the adjacent flow channel. It can be noted that despite accounting for the flow distribution, the HTC on each sides do not coincide on a single correlation. It is therefore likely that side A experience an added enhances in the HTC due to the impinging oil on that surface. This effect is likened to that experienced on the pressure and suction sides of gas turbine blades. Non – dimensional correlations for the pressure side (Side A) and suction side (Side B) of the pole pieces was presented and compared to existing correlations for laminar flow in pipes. It was shown that existing laminar correlations under-predict the values of the heat transfer coefficient when applied to the settings of a directly oil cooled electrical machine.

ACKNOWLEDGEMENTS

The authors would like to thank Mr. Robin Vincent, Mr. Cleveland Williams and Mr. Maurice Keble Smith for their input during the manufacturing of the test box and setting up of the experiment. The input of Mr. Trevor Godfrey in the manufacturing of the thin film gauges is appreciated. Funding and support from Seifert Systems Malta Ltd. is also acknowledged and appreciated.

REFERENCES

Airoldi, G., Ingram, G., Mahgamov, K., Bumby, J., Dominy, R., Brown, N., Mebarki, A., Shanel, M., "Computations on Heat Transfer in Axial Flux Permanent Magnet Machines", Proceedings of the 2008 Int. conf. on Electrical Machines, (ICEM 2008), pp. 1-6, September, 2008, Vilamoura, Portugal.

APTI435. *Atmospheric Sampling Course; Theory and Calibration Procedures for the Use of a Rotameter,* http://www.epa.gov/eogapti1/Materials/APTI%20435%20student/Student%20Manual/Appendix_F_no%20TOC-cover_MRpf.pdf, accessed on: 6/13, 2012.

Boglietti, A., Cavagnino, A., Staton, D., Shanel, M., Mueller, M., Mejuto, C., *Evolution and Modern Approaches of Thermal Analysis of Electrical Machines*, IEEE. Trans. on Ind. Electron., Vol. 56, No. 3, Mar. 2009, pp. 871-882

Camilleri, R., Howey, D.A., McCulloch, M.D., 2012, *Thermal limitations in air-cooled axial flux in-wheel motors for urban mobility vehicles: A preliminary analysis*, in The 2012 Electrical Systems for Aircraft, Railway and Ship Propulsion, pp. 1-8.

Camilleri, R., McCulloch, M.D., 2015, Investigation of an integrated evaporative cooling mechanism for an outer rotor permanent magnet machine, Heat Transfer Engineering, Vol. 36, No. 14-15, pp. 1192-1202.

Camilleri, R., Howey, D.A., McCulloch, M.D., Predicting the Temperature and Flow Distribution in a Direct Oil-Cooled Electrical Machine with Segmented Stator, 2015, (accepted for publication in IEEE Transactions on Industrial Electronics)

Collins, M., Chana, Kam., Povey, T., New Technique for the fabrication of miniature thin film heat flux gauges, Meas. Sci. Technol., Vol. 26, pp.

Howey, D.A., "Thermal design of air-cooled axial flux permanent magnet machines", Doctoral Thesis, Imperial College London, UK, 10 March, 2010

Mellor, P.H., Roberts, D., Turner, D.R., *Lumped parameter thermal model for electrical machines of TEFC design*, IEE Proceedings-B, Vol. 138, No. 5, Sept. 1991, pp. 205-218.

Oldfield, M.L., 2008, Impulse response processing of transient heat transfer gauge signals, J. turbomach, Vol. 130, pp.

ISA-RP16.6-1961. *Methods and Equipment for Calibration of Variable Area Meters; Recommended Practice,* http://www.isa.org/Content/Microsites121/Standards_and_Practices_Department_Board/Home119/Ballots/RP_166.pdf, accessed on: 13/6, 2012.

Wrobel, R., Vainel, G., Copeland, C., Duda, T., Staton, D., Mellor, P., Investigation of a Mechanical Loss Components and Heat Transfer in an Axial Flux PM Machine, 2015, (accepted for publication in IEEE Transactions on Industry Applications)